Available online at www.sciencedirect.com
ScienceDirect
Journal of Power Sources 166 (2007) 514–518
JOURNAL OF POWER SOURCES
www.elsevier.com/locate/jpowsour

Short communication

Preparation and rate capability of $Li_4Ti_5O_{12}$ hollow-sphere anode material

Chunhai Jiang [a], Yong Zhou [b], Itaru Honma [a], Tetsuichi Kudo [a], Haoshen Zhou [a,*]

[a] *Energy Technology Research Institute, National Institute of Advanced Industrial Science and Technology (AIST), 1-1-1, Umezono, Tsukuba, Ibaraki 305-8568, Japan*
[b] *Nanoarchitectonics Research Center, National Institute of Advanced Industrial Science and Technology (AIST), 1-1-1, Higashi, Tsukuba, Ibaraki 305-8565, Japan*

Received 5 December 2006; received in revised form 18 January 2007; accepted 20 January 2007
Available online 2 February 2007

Abstract

Spinel lithium titanate, $Li_4Ti_5O_{12}$, with novel hollow-sphere structure was fabricated by a sol–gel process using carbon sphere as template. The effect of the hollow-sphere structure as well as the wall thickness on the Li storage capability and high rate performance was electrochemically evaluated. High specific capacity, especially better high rate performance was achieved with this $Li_4Ti_5O_{12}$ hollow-sphere electrode material with thin wall thickness. It is believed that this macroporous hollow-sphere structure has shortened the Li diffusion distance, increased the contact area between $Li_4Ti_5O_{12}$ and electrolyte, and also led to better mixing of the active material with AB. All these factors have resulted in the good rate capability of the hollow-sphere structured $Li_4Ti_5O_{12}$ electrode material.

Keywords: Spinel $Li_4Ti_5O_{12}$; Hollow sphere; Li-ion battery; Rate capability

1. Introduction

The spinel lithium titanate, $Li_4Ti_5O_{12}$, has attracted great interest as anode material of rechargeable lithium batteries because of its unique characteristics, such as the 'zero-strain' effect and the flat Li insertion voltage at about 1.55 V versus Li [1–5]. Upon Li insertion, the expansion of the unit cell of $Li_4Ti_5O_{12}$ is almost negligible [3], which may enable a stable cycle life. The high Li insertion potential may stabilize most of the electrolytes and organic solvents since the reduction of electrolytes normally cannot occur at such a high potential. Additionally, $Li_4Ti_5O_{12}$ also has excellent lithium ion mobility [4], hence promising for high rate battery applications.

To develop high rate lithium storage devices, highly divided active materials and high contact area between the active materials and electrolyte are usually two basic requirements [6]. However, in most of previous works, $Li_4Ti_5O_{12}$ powders were fabricated by the high-temperature solid-state reaction method (typically firing at 800–1000 °C for 12–24 h) [1–5]. This method will inevitably yield micron-sized or submicron-sized products even after a post milling step. Although several sol–gel processes were suggested [7–11], high-temperature calcination was always necessary to improve the phase purity [7,8] and electrochemical performance [9]. This makes the fabrication of nano-sized $Li_4Ti_5O_{12}$ rather difficult. In a recent work, Kavan and Grätzel [12] reported a very excellent high rate performance in a nanocrystalline thin-film $Li_4Ti_5O_{12}$ electrode even at a charging rate as high as 250 C. This indicates that nano-sized $Li_4Ti_5O_{12}$ electrode material is truly beneficial for the rate capability of Li-ion batteries.

Another method to improve the rate performance of Li-ion battery is to increase the contact area between the active materials and electrolyte, hence making the Li insertion/extraction more sufficiently. For this purpose, keeping more porosity and less agglomeration of the active materials through assembling them into three-dimensional (3D) architecture seems to be an effective way. Recently Sorensen et al. [13] demonstrated that 3D ordered macroporous $Li_4Ti_5O_{12}$ electrode could deliver

* Corresponding author. Tel.: +81 29 861 5795; fax: +81 29 861 5799.
E-mail address: hs.zhou@aist.go.jp (H. Zhou).

0378-7753/$ – see front matter © 2007 Elsevier B.V. All rights reserved.
doi:10.1016/j.jpowsour.2007.01.065

excellent high rate capacity if carefully controlling the wall thickness. Based on a similar idea, recently we successfully fabricated micron-sized $Li_4Ti_5O_{12}$ hollow spheres with thin wall thickness by a sol–gel process using carbon spheres as template. Significant improvement of the rate capability towards Li insertion/extraction was confirmed in the hollow-sphere structured $Li_4Ti_5O_{12}$ electrode in comparison to the densely agglomerated $Li_4Ti_5O_{12}$ electrode with the similar primary grain size (ca. 100 nm). In this communication, the synthesis and high rate Li storage capability of $Li_4Ti_5O_{12}$ hollow spheres will be reported.

2. Experimental details

2.1. Preparation of carbon spheres

Carbon spheres (CS) with diameters ranging from 500 nm to 2 μm were prepared by hydrothermal treatment of 0.5 M glucose aqueous solution in a teflon-lined autoclave at 180 °C for 20 h, according to the report of Sun et al. [14]. The surface of the carbon spheres has a distribution of –OH and –C=O groups. When the carbon spheres are homogeneously dispersed in the starting sol, a homogenous gel layer containing Ti and Li cations will be coated on them. After burning out the carbon spheres, $Li_4Ti_5O_{12}$ hollow spheres can thus be fabricated.

2.2. Preparation of $Li_4Ti_5O_{12}$ hollow spheres

$Li_4Ti_5O_{12}$ hollow spheres were fabricated from titanium tetraisopropoxide (TTIP), $[Ti(OCH(CH_3)_2)_4]$ (Wako), and lithium acetate dihydrate ($LiCH_3CO_2{\cdot}2H_2O$) (Wako), by a sol–gel process using the as-prepared carbon spheres as template. This sol–gel process has been proven of a facile process to produce well mixed lithium and titanium oxides [7,8]. Typically, 0.1 or 0.2 g as-prepared CS was dispersed in 10 g ethanol by ultrasonic vibrating and magnetic stirring. 1.02 g (for 0.1 g CS) or 0.5 g (for 0.2 g CS) $LiCH_3CO_2{\cdot}2H_2O$ was dissolved in above solutions under magnetic stirring. These different loading amounts of CS were designed to control the wall thickness of the hollow spheres. TTIP was added to these solutions drop wise while keeping the mole ratio of Li:Ti = 1:1. With continuously stirring at room temperature, gels were formed, which were further dried in vacuum at 60 °C. To make a comparison, a sample without addition of CS was also prepared by the same sol–gel process, named as pure. The dried precursors were ground and sintered at 700 or 750 °C for 1–2 h in air to complete the phase transformation. The two kinds of lithium titanate hollow spheres were named as LTHS-1 (for 0.1 g CS) and LTHS-2 (for 0.2 g CS), respectively, to simplify the description. The phase purity and microstructure of the synthesized powders were studied by XRD and scanning electron microscope (SEM).

2.3. Electrochemical characterizations

The charge–discharge capacities were measured with a beaker-type three-electrode cell. To make the working electrode, 70 wt.% $Li_4Ti_5O_{12}$, 20 wt.% acetylene black (AB) carbon and 10 wt.% teflon (poly(tetrafluoroethylene)) binder were mixed and ground into a paste. The prepared paste was spread uniformly on a thin nickel sheet (100 mesh) using the doctor-blade method. The working electrode was dried at 105 °C in vacuum overnight before cell assembly. Li metal on nickel mesh was used as counter and reference electrodes. The electrolyte was 1 M $LiClO_4$ in (EC + DEC) (EC/DEC = 1/1, v/v). The cell assembly was carried out in a glove box filled with high purity argon gas. Galvanostatic discharge–charge measurement was performed in a potential range of 1.0–2.7 V versus Li under different current densities. The specific capacity and current density were based on the active material ($Li_4Ti_5O_{12}$) only, which was typically 1.5–2 mg per electrode.

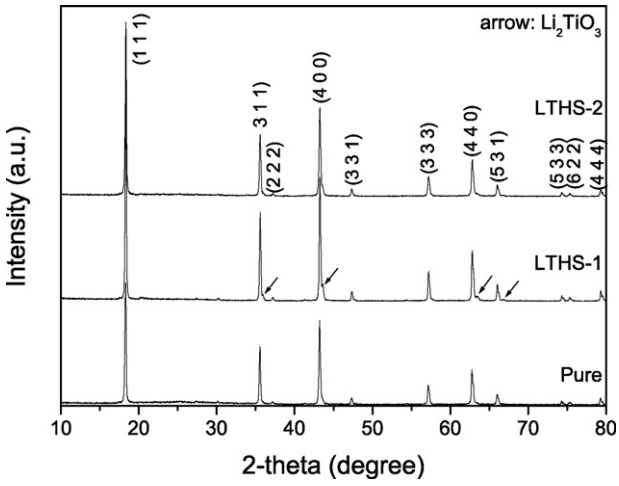

Fig. 1. XRD patterns of the synthesized $Li_4Ti_5O_{12}$ powders with different microstructures.

3. Results and discussion

The colors of the synthesized powders are white, indicating that (1) the CS has been burned out during the heat treatment, and (2) all the samples are insulators. This is different from the results of Zaghib and coworkers [15]. In their work, the powders with carbon addition appeared as grey color even after heat treatment, suggesting that Ti^{3+} or residual carbon might exist.

The X-ray diffraction patterns of the synthesized powders are shown in Fig. 1. All the sharp diffraction peaks can be indexed on the basis of a cubic spinel structure, $Li_4Ti_5O_{12}$ (JCPDS file no. 26-1198). This suggests that high purity $Li_4Ti_5O_{12}$ can be prepared by firing the sol–gel derived precursors at 700–750 °C for only 1–2 h. In all these samples, a small amount of Li_2TiO_3 phase can be traced, as marked by arrow in Fig. 1. In preliminary studies we found that TiO_2 and Li_2TiO_3 phases would coexist with the main $Li_4Ti_5O_{12}$ phase when the sintering temperature was lower than 600 °C. With increasing the heat treatment temperature, TiO_2 or Li_2TiO_3 would disappear depending on the starting composition, Li rich or Ti rich. The Li rich composition and also the low heat treatment temperature may account for the small amount of impurity Li_2TiO_3 phase in our samples.

Fig. 2 shows the SEM images of the synthesized pure (Fig. 2a and b), LTHS-1 (Fig. 2c and d) and LTHS-2 (Fig. 2e and f) powders with low and high magnification, respectively. Generally,

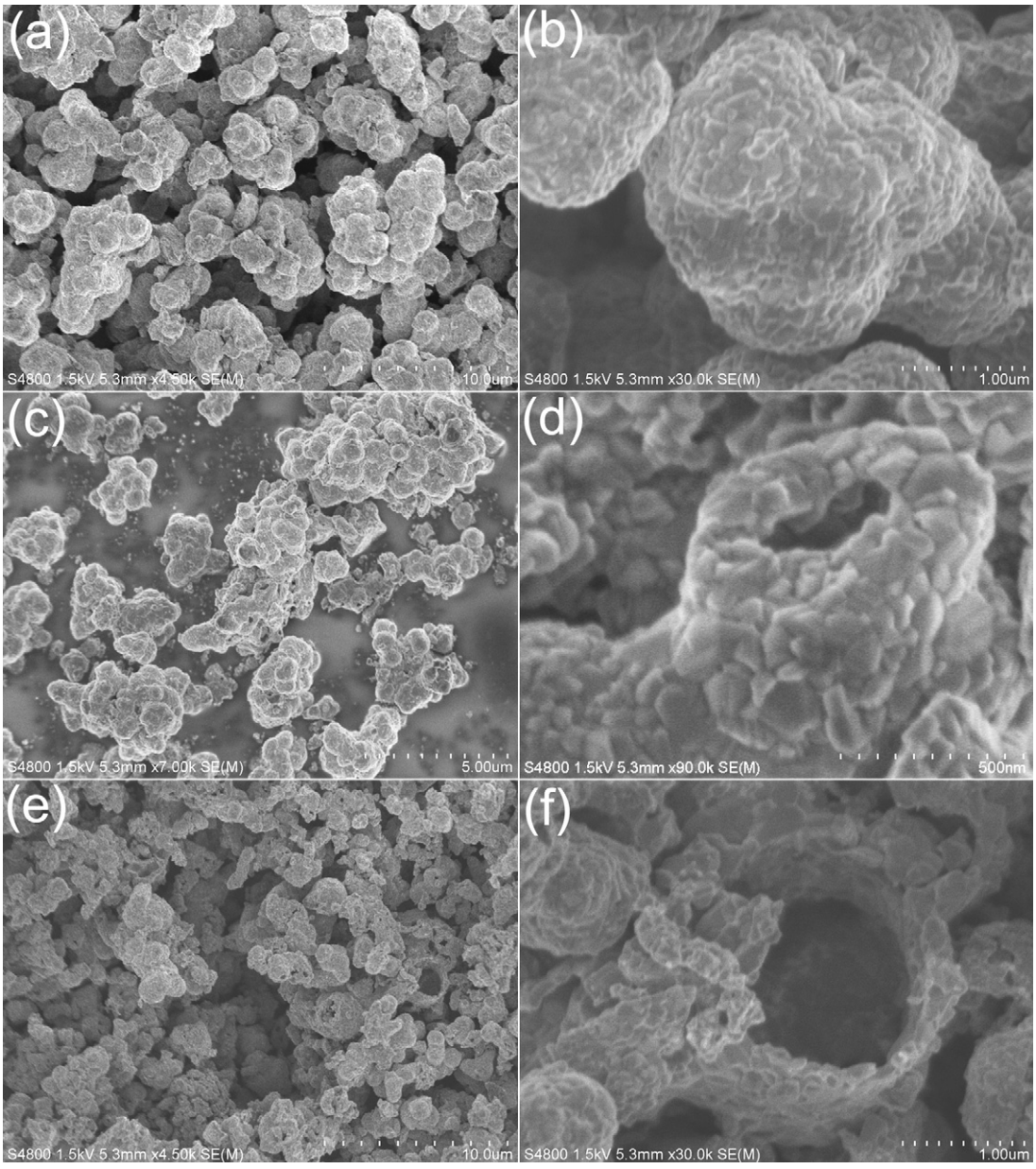

Fig. 2. Low and high magnification SEM images of the synthesized $Li_4Ti_5O_{12}$ powders with different microstructures, (a) and (b) pure, (c) and (d) LTHS-1, and (e) and (f) LTHS-2.

the crystallite size of $Li_4Ti_5O_{12}$ is about 100 nm in all these samples. These fine $Li_4Ti_5O_{12}$ powders could be attributed to the sol–gel process in which an atomic level mixing of elements was achieved. The short sintering time was also important to prevent the grain growth. As is seen in Fig. 2a and b, the pure sample shows very densely agglomerated particles with diameters of ca. 1–2 μm. For these densely packed particles, we assume that the electrolyte can only contact with the $Li_4Ti_5O_{12}$ grains resided at or near the outer surface. The $Li_4Ti_5O_{12}$ grains inside the particles might be inactive especially when being cycled at high current densities due to the increased Li diffusion length. LTHS-1 also shows micron-sized particles of ca. 1 μm in diameter. However, from the magnified image, Fig. 2d, we can clearly see that the micron-sized particles are actually hollow spheres but with thick wall. The wall of these hollow spheres consists of about two grains, i.e., is about 200 nm thick. This thick wall should be ascribed to the lower loading amount of CS in the starting solution. By increasing the loading weight of CS (sample LTHS-2), the wall of the hollow spheres was reduced to one grain thick, i.e., ca. 100 nm, see Fig. 2e and f. Macroporous powders with well assembled $Li_4Ti_5O_{12}$ primary grains were thus obtained. It is believed that these micron-sized hollow spheres with thin wall thickness may facilitate Li insertion/extraction due to the nano-sized diffusion distance and large contact area between the active material and electrolyte.

The specific capacities of these samples were determined by discharge–charge test at constant current density. Fig. 3 plots the first and second discharge and charge curves of these samples at a current rate of $0.1\,A\,g^{-1}$ (ca. 0.57 C, $1\,C = 175\,mA\,g^{-1}$). The pure and LTHS-1 samples show similar first and second

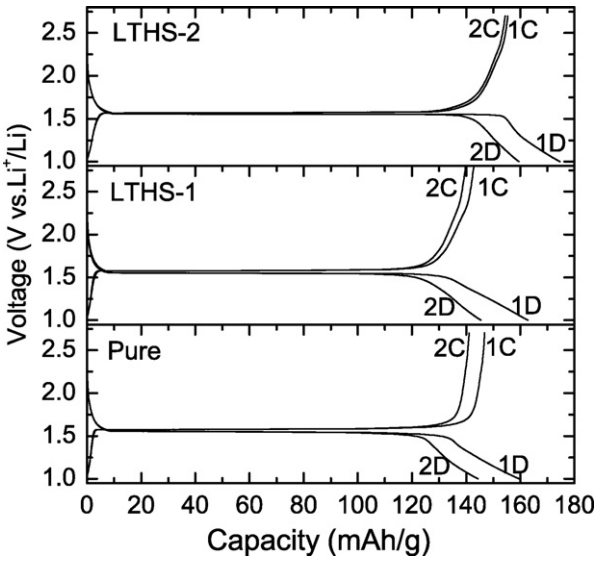

Fig. 3. The first and second discharge and charge curves of $Li_4Ti_5O_{12}$ powders with different microstructures cycled at 0.1 A g^{-1}.

discharge capacities of ca. 160 and 145 mAh g^{-1}, respectively. This indicates that at a relatively low current density, 0.1 A g^{-1}, LTHS-1 shows a similar electrochemical performance as the pure sample due to the thick wall of the hollow spheres. However, by decreasing the wall thickness and increasing the porosity, LTHS-2 delivers a much improved capacity. For example, the discharge capacities of LTHS-2 are 175 mAh g^{-1} at the first cycle and 159 mAh g^{-1} at the second cycle, respectively, suggesting that the lithiation/delithiation processes were greatly facilitated by decreasing the lithium diffusion distance and increasing the contact area between $Li_4Ti_5O_{12}$ and electrolyte.

The cycle performance of these samples at 0.1 A g^{-1} is given in Fig. 4. As is seen in this figure, all these samples show an irreversible capacity of about 10% at the first cycle. This might be ascribed to the low crystallinity of our $Li_4Ti_5O_{12}$ samples due to the short sintering time and low sintering temperature. This can also be identified from Fig. 3 that the discharge curves in a potential range of 1.50–1.0 V are not as sharp as that of the high-

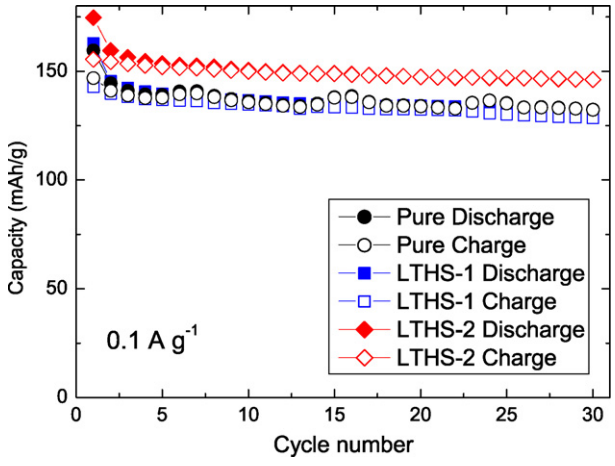

Fig. 4. Cycling performance of the pure, LTHS-1 and LTHS-2 electrodes at a current rate of 0.1 A g^{-1}.

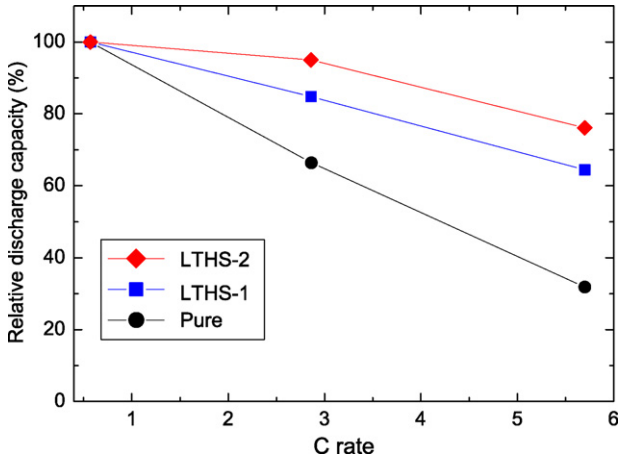

Fig. 5. Effect of current rate on the relative discharge capacities of the pure, LTHS-1 and LTHS-2 samples. The data was obtained by normalizing the second discharge capacities at different current rates to that at 0.57 C.

temperature sintered samples [1–5]. However, after the initial capacity loss, all these samples show very high coulombic efficiency and capacity retention upon cycling. LTHS-2 exhibits the highest capacity among all these samples. A discharge capacity of 146 mAh g^{-1} was maintained after 30 cycles.

To evaluate the rate capability of the $Li_4Ti_5O_{12}$ powders with different microstructures, we have also measured the specific discharge–charge capacities at higher current rates. Fig. 5 plots the relative discharge capacities of three samples as a function of the discharge–charge C rate. The discharge capacity determined at 0.57 C (0.1 A g^{-1}) was taken as standard. Clearly, the rate performance was improved in the turn of pure, LTHS-1 and LTHS-2 samples. Moreover, the advantage of the hollow-sphere electrode material on the high rate capability was highlighted with increasing the current rate. For example, at 2.86 and 5.7 C, the second discharge capacities of the pure sample were only 96 and 46 mAh g^{-1}, being only 66% and 31.8% of the capacity at 0.57 C, respectively; whereas these values of LTHS-2 were 151 and 121 mAh g^{-1}, being 95% and 76% of the capacity at 0.57 C, respectively. These results demonstrated that using $Li_4Ti_5O_{12}$ hollow-sphere electrode material especially with thin wall thickness had significantly improved the rate capability of lithium ion cells.

It should be pointed out that the rate capability of our hollow-sphere $Li_4Ti_5O_{12}$ anode is inferior to that reported by Nakahara et al. [16], in which ball milled fine $Li_4Ti_5O_{12}$ particles could retain 86% of the capacity at 0.15 C when being cycled at 10 C. One possible reason for this difference might be the partial contact of $Li_4Ti_5O_{12}$ primary grains in hollow spheres with AB due to the hollow-sphere structure, which limited the electronic conductivity, in turn the rate capability. The different crystallinity, phase purity and morphology between our samples and that prepared by Nakahara et al. [16] might have also possibly caused such a difference.

As seen in Fig. 5, the difference of capacity between three samples is not large at low current rate. As discussed in ref. [13], at low current density, more sufficient Li insertion/extraction can be realized even in bulk materials, which mini-

mized the difference between the lithium storage capabilities of different samples. However, with increasing the current rate, the transportation of Li ions and electrons in the solid-state electrode material becomes a limiting factor to the lithium insertion/extraction. The hollow-sphere structure of $Li_4Ti_5O_{12}$ may have two merits to account for the better high rate performance than the solid spheres. First, about 100 nm-sized $Li_4Ti_5O_{12}$ grains were assembled on the wall of the hollow spheres. All these fine $Li_4Ti_5O_{12}$ grains were exposed to the electrolyte, hence greatly reducing the Li diffusion distance and increasing the contact area between $Li_4Ti_5O_{12}$ and electrolyte. By contrast, besides the low specific surface area, Li ions could not reach the $Li_4Ti_5O_{12}$ grains inside the densely agglomerated micron-sized particles in the pure sample when the discharge–charge current rate was high. Only the $Li_4Ti_5O_{12}$ grains at or near the outer surface of the micron-sized particles could be active during discharge–charge. This will inevitably decrease the specific capacity. Second, since $Li_4Ti_5O_{12}$ is electronic insulator, conducting assistant material (AB in this study) has to be mixed evenly with the active material to give good electronic conductivity. Compared with the densely packed $Li_4Ti_5O_{12}$ particles in the pure sample, more $Li_4Ti_5O_{12}$ primary grains can contact with AB, hence improving the electronic conductivity. This may also help to improve the high rate performance. Since aggregation is a common shortage of nanopowders, the hollow-sphere structured materials may have advantages as electrode over highly aggregated nanoparticles in order to improve the rate capability. However, as already being pointed, in comparison to evenly dispersed fine particles, the advantage of the hollow-sphere structured electrode materials on high rate performance would be limited.

4. Conclusion

$Li_4Ti_5O_{12}$ hollow spheres with thin wall thickness (ca. 100 nm) were fabricated by a simple sol–gel process using carbon spheres as template. In comparison to the densely agglomerated micron-sized particles, the $Li_4Ti_5O_{12}$ hollow-sphere material shows higher lithium storage capacity, especially at higher current rates. It is believed that the short Li diffusion distance, large contact area between $Li_4Ti_5O_{12}$ and electrolyte, and also the well mixing of $Li_4Ti_5O_{12}$ with AB have increased both the efficiency of Li ion and electronic conductivity, hence the rate capability. Our process is a versatile method, which can possibly be applied to other lithium intercalation materials.

Acknowledgements

This work is financially supported by the New Energy and Industrial Technology Development Organization (NEDO). C.H. Jiang thanks Drs. E. Hosono and M.D. Wei for their help on the experiments.

References

[1] K.M. Colbow, J.R. Dahn, R.R. Haering, J. Power Sources 26 (1989) 397.
[2] E. Ferg, R.J. Gummov, A. de Kock, M.M. Thacheray, J. Electrochem. Soc. 141 (1994) L147.
[3] T. Ohzuku, A. Ueda, N. Yamamoto, J. Electrochem. Soc. 142 (1995) 1431.
[4] S. Takai, M. Kamata, S. Fujine, K. Yoneda, K. Kanda, T. Esata, Solid State Ionics 123 (1999) 165.
[5] K. Zaghib, M. Simoneau, M. Armand, M. Gauthier, J. Power Sources 81–82 (1999) 300.
[6] A.S. Arico, P. Bruce, B. Scrosati, J.M. Tarascon, W. Van Schalkwijk, Nature Mater. 4 (2005) 366.
[7] S. Bach, J.P. Pereira-Ramos, N. Baffier, J. Power Sources 81–82 (1999) 273.
[8] S. Bach, J.P. Pereira-Ramos, N. Baffier, J. Mater. Chem. 8 (1998) 251.
[9] C.M. Shen, X.G. Zhang, Y.K. Zhou, H.L. Li, Mater. Chem. Phys. 78 (2002) 437.
[10] Y.K. Rho, K. Kanamura, M. Fujisaki, J. Hamagami, S. Suda, T. Umegaki, Solid State Ionics 151 (2002) 151.
[11] Y.J. Hao, Q.Y. Lai, J.Z. Lu, H.L. Wang, Y.D. Chen, X.Y. Ji, J. Power Sources 158 (2006) 1358.
[12] L. Kavan, M. Grätzel, Electrochem. Solid-State Lett. 5 (2002) A39.
[13] E.M. Sorensen, S.J. Barry, H.K. Jung, J.R. Rondnelli, J.T. Vaughey, K.R. Poeppelmeier, Chem. Mater. 18 (2006) 482.
[14] X.M. Sun, Y.D. Li, Angew. Chem. Int. Ed. 43 (2004) 3827.
[15] A. Guerfi, S. Sevigny, M. Lagace, P. Hovington, K. Kinoshita, K. Zaghib, J. Power Sources 119–121 (2003) 88.
[16] K. Nakahara, R. Nakajima, T. Matsushima, H. Majima, J. Power Sources 117 (2003) 31.